# Tracking of Time-Variant Radio Propagation Paths using Particle Filtering

Yin, Xuefeng; Steinböck, Gerhard; Kirkelund, Gunvor; Pedersen, Troels; Blattnig, Peter; Jaquier, Alain; Fleury, Bernard Henri

*Published in:*
IEEE International Conference on Communications, 2008. ICC '08

*DOI (link to publication from Publisher):*
10.1109/ICC.2008.180

*Publication date:*
2008

*Document Version*
Publisher's PDF, also known as Version of record

This full text paper was peer reviewed at the direction of IEEE Communications Society subject matter experts for publication in the ICC 2008 proceedings.

# Tracking of Time-Variant Radio Propagation Paths using Particle Filtering

Xuefeng Yin[1], Gerhard Steinböck[1,4], Gunvor Elisabeth Kirkelund[1], Troels Pedersen[1],
Peter Blattnig[2], Alain Jaquier[2], and Bernard H. Fleury[1,3]
[1]Section Navigation and Communications, Department of Electronics Systems,
Aalborg University, DK-9220 Aalborg, Denmark
[2] Federal Department for Defence, Civil Protection and Sports,
armasuisse, science and technology, Switzerland.
[3]Forschungszentrum Telekommunikation Wien (ftw.), Vienna, Austria
[4] Austrian Research Centers GmbH - ARC, smart systems Division, Vienna, Austria
Email: xuefeng@es.aau.dk

***Abstract*— In this contribution a low-complexity particle filtering algorithm is proposed to track the parameters of time-variant propagation paths in multiple-input multiple-output (MIMO) radio channels. A state-space model is used to describe the path evolution in delay, azimuth of arrival, azimuth of departure, Doppler frequency and complex amplitude dimensions. The proposed particle filter (PF) has an additional resampling step specifically designed for wideband MIMO channel sounding, where the posterior probability density functions of the path states is usually highly concentrated in the multi-dimensional state space. Preliminary investigations using measurement data show that the proposed PF can track paths stably with a small number of particles, e.g. 5 per path, even in the case where the paths are undetected by the conventional SAGE algorithm.**

***Index Terms*— Radio propagation channel, sequential Bayesian estimation, particle filter, state-space model, and maximum-likelihood estimation.**

## I. Introduction

The response of the radio propagation channel can be modelled as a superposition of multiple path components. Each component is contributed by an electromagnetic wave propagating along a path between the transmitter (Tx) and the receiver (Rx). One path can be characterized by various dispersion parameters, such as delay, direction of arrival (DoA), direction of departure (DoD), polarization matrix, as well as Doppler frequency. In time-variant scenarios, due to long-term/large-scale fluctuations, these path parameters may vary with time.

Recently, the temporal behavior of propagation paths have gained much attention [1], [2]. In [1] the time-variant characteristics of path parameters are considered as an additional degree of freedom for path clustering. In [2], the evolution of clusters of paths is illustrated using measurement data. In these works, the path evolution characteristics are obtained indirectly from the path parameter estimates computed from individual observation snapshots. The used estimation methods, e.g. the SAGE algorithm [2] and the Unitary ESPRIT [1], are derived under the assumption that the path parameters in different observation snapshots are independent. This (unrealistic) assumption results in a "loss of information" in the estimation of the path evolution in time. Furthermore, due to model-order mismatch and heuristic settings in these algorithms, such as the (usually fixed) dynamic range, a time-variant path may remain undetected in some snapshots. As a result, a time-variant path can be erroneously considered as several paths. These effects influence the performance of clustering algorithms and the effectiveness of the channel models derived based on these results. It is therefore of great importance to use appropriate algorithms to estimate the temporal characteristics of paths directly.

In recent years some methods have been proposed to track time-variant paths for multiple-input multiple-output (MIMO) channel sounding [3], [4], [5]. In [3] recursive expectation-maximization (EM) and recursive space-alternating generalized EM (SAGE)-inspired algorithms have been proposed for tracking of the azimuths of arrival (AoAs) of paths. In [4] and [5], the extended Kalman filter (EKF) is derived for tracking of the delays, DoAs, DoDs and complex amplitudes of time-variant paths. These algorithms are applicable in the case where the linear approximation of the non-linear observation model is accurate. In cases where the path parameters fluctuate dramatically, the linear approximation based on Taylor-series expansions is so inaccurate that "loss of track" errors may occur. Furthermore, the parameter updating steps in these algorithms require calculation of the second-order derivatives of the received signal with respect to (w.r.t.) the path parameters. In channel sounding, these derivatives are computed numerically using the system response gathered from calibration measurements. In the presence of calibration errors, these derivatives may be erroneous and cause significant performance degradation.

In this contribution, we propose to use a sequential Monte-Carlo method, i.e. a so-called "particle filter (PF)", to track the parameters of time-variant paths. Differing from the EKF and the recursive EM and SAGE-inspired algorithms, the PF can be applied when the observation model is nonlinear. Furthermore, it does not require the numerical computation of derivatives.

The organization of the paper is as follows. Section II presents the state-space model. In Section III, the framework of the proposed PF is formulated. Section IV describes the preliminary experimental results of applying the PF to track paths using measurement data. Conclusive remarks are made in Section V.

## II. Signal Model

In this section, we introduce the state space model describing the time-evolving path parameters, and the observation

This work was supported by the Federal Department for Defence, Civil Protection and Sports, armasuisse, science and technology, Switzerland.

model for the received signal in the Rx of the sounding equipment. For simplicity of the presentation, these models are discussed while considering a single-path scenario. Extension of these models to multiple-path scenarios is straightforward.

### A. State-Space Model

We consider a scenario where the environment consists of time-variant specular paths. The parameters of a path are the delay $\tau$, the azimuth of departure (AoD) $\phi_1$, the AoA $\phi_2$, the Doppler frequency $\nu$, the rates of change of these parameters that are denoted by $\Delta\tau$, $\Delta\phi_1$, $\Delta\phi_2$, and $\Delta\nu$ respectively, as well as the complex amplitude $\alpha$. The $k$th observation of the state vector of a path is defined as

$$\boldsymbol{\Omega}_k = [\boldsymbol{P}_k^{\mathrm{T}}, \boldsymbol{\alpha}_k^{\mathrm{T}}, \boldsymbol{\Delta}_k^{\mathrm{T}}]^{\mathrm{T}}, \tag{1}$$

where $[\cdot]^{\mathrm{T}}$ denotes the transpose operation, $\boldsymbol{P}_k \doteq [\tau_k, \phi_{1,k}, \phi_{2,k}, \nu_k]^{\mathrm{T}}$ represents the "position" parameter vector, $\boldsymbol{\Delta}_k \doteq [\Delta\tau_k, \Delta\phi_{1,k}, \Delta\phi_{2,k}, \Delta\nu_k]^{\mathrm{T}}$ denotes the "rate-of-change" parameter vector, and $\boldsymbol{\alpha}_k \doteq [|\alpha_k|, \arg(\alpha_k)]^{\mathrm{T}}$ is the amplitude vector with $|\alpha_k|$ and $\arg(\alpha_k)$ representing the magnitude and the argument of $\alpha_k$ respectively. The state vector $\boldsymbol{\Omega}_k$ is modelled as a Markov process, i.e.

$$p(\boldsymbol{\Omega}_k|\boldsymbol{\Omega}_{1:k-1}) = p(\boldsymbol{\Omega}_k|\boldsymbol{\Omega}_{k-1}), \quad k \in [1, \ldots, K], \tag{2}$$

where $\boldsymbol{\Omega}_{1:k-1} \doteq \{\boldsymbol{\Omega}_1, \ldots, \boldsymbol{\Omega}_{k-1}\}$ is a sequence of state values from the 1st to the $(k-1)$th observation, and $K$ denotes the total number of observations. The transition of $\boldsymbol{\Omega}_k$ w.r.t. $k$ is modelled as

$$\underbrace{\begin{bmatrix}\boldsymbol{P}_k\\ \boldsymbol{\alpha}_k\\ \boldsymbol{\Delta}_k\end{bmatrix}}_{\boldsymbol{\Omega}_k} = \underbrace{\begin{bmatrix}\boldsymbol{I}_4 & \boldsymbol{0}_{4\times2} & T_k\boldsymbol{I}_4\\ \boldsymbol{J}_k & \boldsymbol{I}_2 & \boldsymbol{0}_{2\times4}\\ \boldsymbol{0}_{4\times4} & \boldsymbol{0}_{4\times2} & \boldsymbol{I}_4\end{bmatrix}}_{\boldsymbol{F}_k \doteq} \underbrace{\begin{bmatrix}\boldsymbol{P}_{k-1}\\ \boldsymbol{\alpha}_{k-1}\\ \boldsymbol{\Delta}_{k-1}\end{bmatrix}}_{\boldsymbol{\Omega}_{k-1}} + \underbrace{\begin{bmatrix}\boldsymbol{0}_{4\times1}\\ \boldsymbol{v}_{\boldsymbol{\alpha},k}\\ \boldsymbol{v}_{\Delta,k}\end{bmatrix}}_{\boldsymbol{v}_k \doteq}, \tag{3}$$

where $\boldsymbol{I}_n$ represents the $n \times n$ identity matrix, $\boldsymbol{0}_{b\times c}$ is the all-zero matrix of dimension $b \times c$,

$$\boldsymbol{J}_k = \begin{bmatrix}0 & 0 & 0 & 0\\ 0 & 0 & 0 & 2\pi T_k\end{bmatrix},$$

and $T_k$ denotes the interval between the starts of the $(k-1)$th and the $k$th observation periods. The vector $\boldsymbol{v}_k$ in (3) contains the driving process in the amplitude vector

$$\boldsymbol{v}_{\boldsymbol{\alpha},k} \doteq [v_{|\alpha|,k},\ v_{\arg(\alpha),k}]^{\mathrm{T}} \tag{4}$$

and in the rate-of-change parameter vector

$$\boldsymbol{v}_{\boldsymbol{\Delta},k} \doteq [v_{\Delta\tau,k},\ v_{\Delta\phi_1,k},\ v_{\Delta\phi_2,k},\ v_{\Delta\nu,k}]^{\mathrm{T}}. \tag{5}$$

The entries $v_{(\cdot),k}$ in (4) and (5) are independent Gaussian random variables $v_{(\cdot),k} \sim \mathcal{N}(0, \sigma^2_{(\cdot)})$.

In this contribution, we consider the case with $T_k = T$, $k \in [1, \ldots, K]$. For notational brevity, we drop the subscript $k$ in $\boldsymbol{F}_k$ in the sequel.

### B. Observation Model

In the $k$th observation period, the discrete-time signals at the output of the $m_2$th Rx antenna when the $m_1$th Tx antenna transmits can be written as

$$\begin{aligned} y_{k,m_1,m_2}(t) = {} & x_{k,m_1,m_2}(t;\boldsymbol{\Omega}_k) + n_{k,m_1,m_2}(t),\\ & t \in [t_{k,m_1,m_2}, t_{k,m_1,m_2} + T),\\ & m_1 = 1, \ldots, M_1,\ m_2 = 1, \ldots, M_2, \end{aligned} \tag{6}$$

where $t_{k,m_1,m_2}$ denotes the time instant when the $m_2$th Rx antenna starts to receive signals while the $m_1$th Tx antenna transmits, $T$ is the sensing duration of each Rx antenna, $M_1$ and $M_2$ represent the total number of Tx antennas and Rx antennas respectively. The signal contribution $x_{k,m_1,m_2}(t;\boldsymbol{\Omega}_k)$ reads

$$\begin{aligned} x_{k,m_1,m_2}(t;\boldsymbol{\Omega}_k) = {} & \alpha_k \exp(j2\pi\nu_k t) c_{1,m_1}(\phi_{k,1}) c_{2,m_2}(\phi_{k,2})\\ & \cdot u(t-\tau_k). \end{aligned} \tag{7}$$

Here, $c_{1,m_1}(\phi)$ and $c_{2,m_2}(\phi)$ represent respectively the response in azimuth of the $m_1$th Tx antenna, and the response in azimuth of the $m_2$th Rx antenna, $u(t-\tau_k)$ denotes the transmitted signal delayed by $\tau_k$. The noise $n_{k,m_1,m_2}(t)$ in (6) is a zero-mean Gaussian process with spectrum height $\sigma_n^2$. For notational convenience, we use the vector $\boldsymbol{y}_k$ to represent all the samples received in the $k$th observation period and $\boldsymbol{y}_{1:k} \doteq \{\boldsymbol{y}_1, \boldsymbol{y}_2, \ldots, \boldsymbol{y}_k\}$ to denote a sequence of observations.

## III. The Particle Filter

From (2) and (6) we see that the received signal $\boldsymbol{y}_k$ depends only on the current state $\boldsymbol{\Omega}_k$ and is conditionally independent of the other states given $\boldsymbol{\Omega}_k$. Utilizing this property, a particle filtering (PF) approach can be used to estimate the posterior probability density function (pdf) $p(\boldsymbol{\Omega}_{1:k}|\boldsymbol{y}_{1:k})$ sequentially [6]. The facts that the parameter space is multi-dimensional[1] and the temporal and spatial observation apertures are large in order to achieve high resolution pose a noticeable challenge when using the PF in wideband MIMO sounding. As a result, the posterior pdf $p(\boldsymbol{\Omega}_{1:k}|\boldsymbol{y}_{1:k})$ is highly concentrated in the parameter space. It is then difficult to "steer" the particle sets to the regions where the probability mass is localized. The proposed PF is specifically designed to solve this problem. In this section we first present the algorithm while considering a single-path scenario, and then discuss the extension of the algorithm for tracking multiple paths.

### A. Initialization of Particle States

We initialize the particle states by using the parameter estimates obtained with the conventional SAGE algorithm [7]. This algorithm is derived based on the assumption that the path parameters at different observation snapshots are independent. In this contribution, we use the PF to track $\boldsymbol{\Omega}_k$ from the 3rd observation period. The vector $\boldsymbol{\Omega}_k^i$ of the $i$th particle has the initial state $\boldsymbol{\Omega}_2^i$. The position parameter vector $\boldsymbol{P}_2^i$ are set to be identical with the parameter estimates obtained with the SAGE algorithm in the 2nd observations. The rate of change parameters are calculated by taking the difference between the SAGE estimates obtained at the 1st and the 2nd observations.

### B. Framework of the PF

When a new observation, say $\boldsymbol{y}_k$, is available, the PF performs the following steps.

***Step 1: Predict the states of particles and calculate importance weights.*** The output from the previous observations are the set $\{\boldsymbol{\Omega}_{k-1}^i, w_{k-1}^i\}$, where $w_{k-1}^i$ denotes the importance weight of the $i$th particle. We first predict the states of all

[1]The parameter space has dimension up to 14 in the specular-path scenario [7] and up to 28 in the dispersive-path scenario [8].

particles for the $k$th observation period. The rate-of-change parameter vector $\boldsymbol{\Delta}_k^i$ is updated as

$$\boldsymbol{\Delta}_k^i = \boldsymbol{\Delta}_{k-1}^i + \boldsymbol{\Delta w}_k^i, \quad i = 1, \ldots, I, \tag{8}$$

where $I$ denotes the total number of particles, and the vector $\boldsymbol{\Delta w}_k^i$ is drawn from a $\mathcal{N}(\mathbf{0}, \boldsymbol{\Sigma}_{\boldsymbol{w}})$ distribution. The diagonal covariance matrix $\boldsymbol{\Sigma}_{\boldsymbol{w}}$ reads

$$\boldsymbol{\Sigma}_{\boldsymbol{w}} = \mathrm{diag}(\sigma_{\Delta\tau}^2, \sigma_{\Delta\phi_1}^2, \sigma_{\Delta\phi_2}^2, \sigma_{\Delta\nu}^2). \tag{9}$$

The values of the diagonal elements $\sigma_{\Delta(\cdot)}^2$ with $(\cdot)$ replaced by $\tau$, $\phi_1$, $\phi_2$ or $\nu$, are predetermined. The position vector $\boldsymbol{P}_k^i$ is calculated as

$$\boldsymbol{P}_k^i = \boldsymbol{P}_{k-1}^i + \boldsymbol{\Delta}_k^i. \tag{10}$$

The complex amplitude $\alpha_k^i$ is computed analytically as

$$\alpha_k^i = \frac{(\boldsymbol{s}_k^i)^{\mathrm{H}} \boldsymbol{y}_k}{\|\boldsymbol{s}_k^i\|^2}, \tag{11}$$

where $(\cdot)^{\mathrm{H}}$ represents the Hermitian transpose, $\|\cdot\|$ denotes the Euclidian norm of the given argument, and the vector $\boldsymbol{s}_k^i$ contains the elements

$$\begin{aligned} s_{k,m_1,m_2}^i(t; \boldsymbol{P}_k^i) = &\exp(j2\pi\nu_k^i t) c_{1,m_1}(\phi_{1,k}^i) c_{2,m_2}(\phi_{2,k}^i) \\ &\cdot u(t - \tau_k^i), t \in [t_{k,m_1,m_2}, t_{k,m_1,m_2} + T). \end{aligned}$$

The importance weights of the particles are calculated as

$$w_k^i = \frac{w_{k-1}^i p(\boldsymbol{y}_k | \boldsymbol{\Omega}_k^i)}{\sum_{i=1}^{I} w_{k-1}^i p(\boldsymbol{y}_k | \boldsymbol{\Omega}_k^i)}, \quad i = 1, \ldots, I \tag{12}$$

with

$$p(\boldsymbol{y}_k | \boldsymbol{\Omega}_k^i) \propto \exp(-\frac{1}{2\sigma_n^2} \|\boldsymbol{y}_k - \alpha_k^i \boldsymbol{s}_k^i\|^2). \tag{13}$$

***Step 2: Additional resampling.*** In wideband MIMO channel sounding, the amount of temporal-spatial samples in one observation period is usually large. As a consequence, significant portions of the posterior pdf $p(\boldsymbol{\Omega}_{1:k} | \boldsymbol{y}_{1:k})$ are concentrated around the modes of the pdf. As the path parameters evolve over time, the particles with predicted states can be too diffuse to "catch" the probability mass. One brute-force solution is to employ a large number of particles. However the resulting complexity prohibits any practical implementation. This problem can be overcome with low complexity using the methods proposed for vision–based robot localization and tracking, e.g. assuming a noise variance higher than its true value, distributing particles either uniformly within a subset of the parameter space [9] or based on multi-hypothesis [10]. However, these methods have the drawback that the weighted particles do not approximate the true posterior density $p(\boldsymbol{\Omega}_{1:k} | \boldsymbol{y}_{1:k})$, and consequently, the estimation results can be artifacts.

In this contribution, we introduce an additional resampling step where two techniques are used for allocation of particles without misinterpreting the posterior density. This step is activated when the importance weights of the particles obtained from (12) are all negligible. The first technique consists in using a part of the observation samples, denoted by $\tilde{\boldsymbol{y}}_k$, to calculate the importance weights. As the number of observation samples in $\tilde{\boldsymbol{y}}_k$ is less than that in $\boldsymbol{y}_k$, the posterior pdf $p(\boldsymbol{\Omega}_k | \tilde{\boldsymbol{y}}_k, \boldsymbol{y}_{1:k-1})$ is less concentrated than the original pdf $p(\boldsymbol{\Omega}_k | \boldsymbol{y}_{1:k})$. Thus, the particles can have higher probability to get significant importance weights.

The second method consists in computing the importance weights as

$$\tilde{w}_k^i \propto \log p(\boldsymbol{y}_k | \boldsymbol{\Omega}_k^i) + \log w_{k-1}^i. \tag{14}$$

The obtained set $\{\boldsymbol{\Omega}_k^i, \tilde{w}_k^i\}$ is an estimate of the function $\log p(\boldsymbol{\Omega}_{1:k} | \boldsymbol{y}_{1:k})$. This function exhibits the same modes as $p(\boldsymbol{\Omega}_{1:k} | \boldsymbol{y}_{1:k})$ but also a wider curvature in the vicinities of the modes. So, the probability to get non-negligible importance weights is enhanced.

Based on these two methods, we propose an additional resampling step, which can be implemented according to the following pseudo code.

**for** $n = 1$ to $N$ **do**
  ***Step 2.1*** Select $\tilde{\boldsymbol{y}}_k^n \in \boldsymbol{y}_k$.
  ***Step 2.2*** Calculate the importance weights $\tilde{w}_k^i$, $i = 1, \ldots, I$.
  **if** $\{\tilde{w}_k^i\}$ contains non-significant values, e.g. less than $\max\{\tilde{w}_k^i\} - 3$, **then**
    ***Step 2.3*** Find the indices $\boldsymbol{A} = \{i^{\mathrm{s}}\}$ of the particles with significant importance weights. Let $D$ denote the number of particles with non-significant weights.
    ***Step 2.4*** Generate $D$ new particles with states drawn from $p(\boldsymbol{\Omega}_k | \boldsymbol{\Omega}_{k-1}^{j(\boldsymbol{A}_d)})$, $d = 1, \ldots, D$. Here, $\boldsymbol{A}_d$ denotes the $d$th element of $\boldsymbol{A}$, and $j(\boldsymbol{A}_d)$ is the index of a particle in the $(k-1)$th observation, from which the $\boldsymbol{A}_d$th particle in the $k$th observation is generated. Replace the particles that have non-significant weights by the new particles.
    ***Step 2.5*** Update the importance weights $w_{k-1}^i$ as

$$w_{k-1}^i = J(i)^{-1} w_{k-1}^{j(i)}, \quad i = 1, \ldots, I, \tag{15}$$

    where $J(i)$ represents the total number of new particles that are generated using the $j(i)$th particle in the $(k-1)$th observation. Go to Step 2.2.
  **end if**
**end for**

***Step 3: Normal resampling.*** The operations performed in this step are similar to those shown in the loop in ***Step 2*** except that the importance weights $\tilde{w}_k^i$ are replaced by $w_k^i$ and the observation $\tilde{\boldsymbol{y}}_k^n$ is substituted with $\boldsymbol{y}_k$.

***Step 4: Estimate the posterior pdf.*** The estimate of the posterior pdf can be approximated with the particle states and importance weights

$$\hat{p}(\boldsymbol{\Omega}_k | \boldsymbol{y}_{1:k}) = \sum_{i=1}^{I} w_k^i \delta(\boldsymbol{\Omega}_k - \boldsymbol{\Omega}_k^i). \tag{16}$$

This pdf estimates can be used to estimate the expectation of a function of $\boldsymbol{\Omega}_k$. For example, in the single-path scenario, the state vector $\boldsymbol{\Omega}_k$ for the path can be estimated as

$$\hat{\boldsymbol{\Omega}}_k = \sum_{i=1}^{I} \boldsymbol{\Omega}_k^i w_k^i. \tag{17}$$

### C. Extension to Multi-Path Scenarios

We considered the case where the paths are dispersive in multiple dimensions. In such a case, the states of different

paths do not coincide with high probability. The paths can then be tracked individually by using separate PFs. The states of the particles in each PF are initialized with the parameter estimates of a specific path. This method is used to track multiple paths in the experimental investigations introduced in Section IV.

## IV. Experimental Investigation

The measurement data was collected using the wideband MIMO channel sounder Elektrobit Propsound CS [11] [12]. This channel sounder operates according to a time-division-multiplexing switching mode [13]. A "measurement cycle" is referred to as the operation where all possible pairs of Tx and Rx antennas are switched once. Measurement data was acquired in a *burst* mode. Each burst has a duration of 16 cycles. Only the data received in the first four cycles in each burst are stored. The sounder setting is reported in Table 1 in [8]. The Tx and the Rx were both equipped with two identical 9-element circular arrays. A diagram of the arrays is shown in Fig. 2 in [8].

We use measurement data acquired in a long corridor. Fig. 1 depicts the premises of the environment and the photographs of the Tx and Rx surroundings. The Rx was fixed at the location marked with a red "⊗" on the map. The Tx was moving towards the Rx with a constant speed along the route marked in red on the map. The Rx was positioned behind a metal door with reinforced glass. There was no line-of-sight path for this scenario. During the measurement, no people were walking. We consider the measurement data collected in 100 consecutive bursts, which has a total time span of 26.93 s. During this period, the Tx moved 7.5 m with a speed of approximately 0.5 m/s. The time-evolution behavior of the propagation paths can be observed from the variation of the power delay profiles (PDPs) of the received signal at different bursts. Fig. 2 shows the average PDPs calculated from the signals received in the burst, for totally 50 consecutive bursts. It can be observed that some peaks of the PDPs move with increasing delay, while others exhibit decreasing delay.

We use the proposed PF to track the parameters of three paths. The parameter estimates of three paths obtained with the SAGE algorithm are applied to initialize the states of the particles. The PF uses 5 particles per path with $\sigma_{\Delta\tau} = 1.5$ ns, $\sigma_{\Delta\phi_1} = \sigma_{\Delta\phi_2} = 4^\circ$ and $\sigma_{\Delta\nu} = 5$ Hz. Notice that in

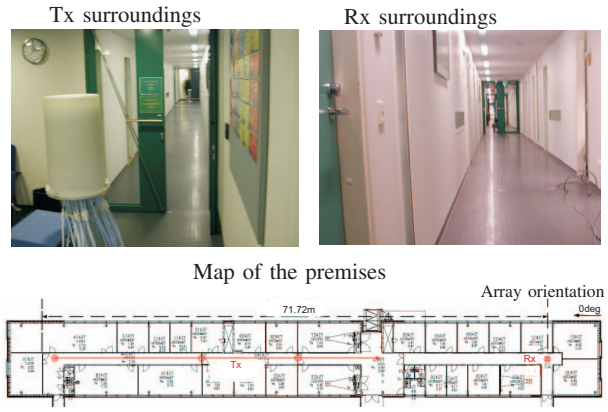


Fig. 1. Photographs and the map of the investigated environment.

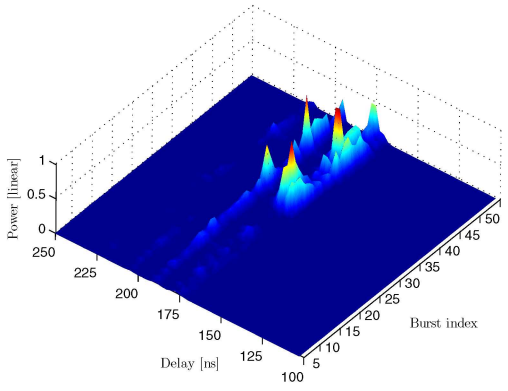


Fig. 2. Average power delay profiles of the received signals computed from 50 bursts.

experimental scenarios where $\sigma_{\Delta\tau}$, $\sigma_{\Delta\phi_1}$, $\sigma_{\Delta\phi_2}$ and $\sigma_{\Delta\nu}$ are unknown, these parameters can be estimated using ray-tracing techniques based on some assumption on the motions of the Tx and the Rx. In this preliminary investigation, for simplicity we select these parameters in such a way that they are very likely larger than the true parameters.

Fig. 3 depicts the trajectories of the parameters of three paths estimated using the PF. In Fig. 3(a), the trajectories of the path delays are overlapped with the PDPs calculated for the 100 bursts. The estimated delay trajectories are consistent with the time-variations of the peaks in the PDPs. In Fig. 3(b)–(f), the parameter estimates of 3 paths obtained with the conventional SAGE algorithm are also depicted. The trajectories estimated with the PF match the SAGE estimates for most of the bursts. Furthermore, the filter is able to track a path even in the interval where the SAGE algorithm failed to detect this path (e.g. Path 3 is undetected by the SAGE algorithm in the burst interval $[82, 100]$).

From Fig. 3(b) we observe that the delay trajectory of Path 3 fluctuates significantly in the burst interval $[80, 90]$. In addition, the Doppler frequency trajectories also exhibit large fluctuations, compared to the SAGE estimates. These effects may be due to the following reasons. First, in this preliminary study the PF is used to track paths individually. In the case where a path is close to other paths in the parameter space, the particles may be steered to a wrong position due to interference. The observation of significant fluctuations in the trajectories can also be due to the inappropriate settings of the variance parameters $\sigma^2_{\Delta(\cdot)}$. For instance, the standard deviation $\sigma_{\Delta\nu}$ of Doppler frequency is specified to be 5 Hz. However, this figure is actually much larger than the true value for all tracked paths. Furthermore, the fluctuations of the trajectories may be caused by the fact that the PF uses only 5 particles for tracking each path. This is probably not enough for accurate estimation of the posterior pdf in the dimensions where the intrinsic resolutions of the sounder are low.

To check whether the path evolution behavior estimated by the PF is sensible, we plot a sketch representing grossly the geometry of the environment in Fig. 4 and reconstruct three possible propagation paths approximately. The table attached in Fig. 4 lists some characteristics of these paths drawn from the geometry. We observe that the paths tracked by the PF from

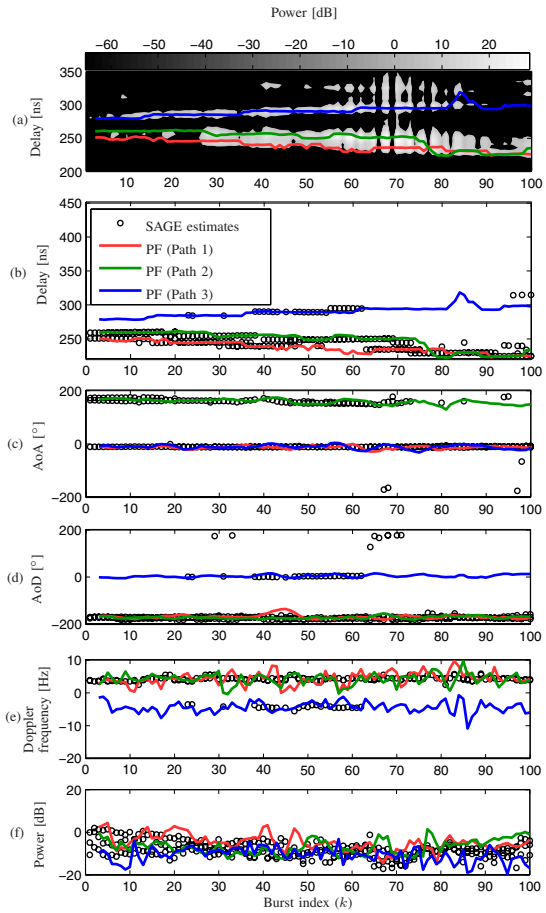


Fig. 3. Performance of the PF in tracking three time-variant paths. The legend given in (b) applies to (a)–(f). In (a), the PDPs computed from 100 bursts are shown in the background.

the measurement data exhibit time-evolution characteristics similar to those of the paths in Fig. 4. This demonstrates that the proposed PF is applicable for the estimation of the time-variant characteristics of propagation paths.

## V. Conclusions

In this contribution, a particle filtering algorithm was designed and used to track the parameters of time-variant propagation paths for channel sounding. The considered parameters include delay, azimuth of arrival, azimuth of departure, Doppler frequency, the rates of change of these parameters, as well as the complex amplitude of individual paths. The particle filter (PF) proposed has an additional resampling step, specifically designed for wideband MIMO channel sounding. The performance of this algorithm was evaluated using measurement data. The proposed PF is capable to track paths stably through the measurement, even in the case when these paths remain undetected with the conventional SAGE algorithm. The estimated time-evolution characteristics are in accordance with the geometry of the investigated environment. Additionally, this proposed PF performs well for a low number of particles per path. The complexity of the PF is even lower than that of the conventional SAGE algorithm. These results demonstrated that the proposed PF is a suitable algorithm for the estimation

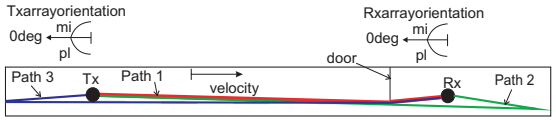


| Path | Delay rate of change | AoA | AoD | Doppler frequency |
|---|---|---|---|---|
| No. 1 | −0.5 ns/burst | 0° | −180° | 8 Hz |
| No. 2 | −0.5 ns/burst | 170° | −180° | 8 Hz |
| No. 3 | +0.5 ns/burst | 0° | 0° | −8 Hz |

Fig. 4. Geometries and characteristics of reconstructed propagation paths in the investigated environment. The approximate values of the AoAs, AoDs and Doppler frequencies computed from the geometrical figure are reported in the table.

of the characteristics of time-variant propagation paths in wideband MIMO channel sounding.

## VI. Acknowledgement

The authors would like to acknowledge Nicolai Czink for providing the measurement data.

## References

[1] M. Kwakkernaat and M. Herben, "Analysis of clustered multipath estimates in physically nonstationary radio channels," in *Proceedings of the 17th IEEE International Symposium on Personal, Indoor and Mobile Radio Communications (PIMRC)*, Athens, Greece, September 2007.

[2] N. Czink, R. Tian, S. Wyne, G. Eriksson, F. Tufvesson, T. Zemen, J. Nuutinen, J. Ylitalo, E. Bonek, and A. Molisch, "Tracking time-variant cluster parameters in MIMO channel measurements: Algorithm and results," in *Proceedings of International Conference on Communications and Networking in China (ChinaCOM)*, Shanghai, China, August 2007.

[3] P. Chung and J. F. Böhme, "Recursive EM and SAGE-inspired algorithms with application to DOA estimation," *IEEE Transactions on Signal Processing*, vol. 53, no. 8, pp. 2664–2677, August 2005.

[4] A. Richter, J. Salmi, and V. Koivunen, "An algorithm for estimation and tracking of distributed diffuse scattering in mobile radio channels," in *Proceedings of the 7th IEEE International Workshop on Signal Processing Advances for Wireless Communications (SPAWC'06)*, 2006.

[5] J. Salmi, A. Richter, and V. Koivunen, "Enhanced tracking of radio propagation path parameters using state-space modeling," in *Proceedings of the 2006 European Signal Processing Conference (EUSIPCO)*, Florence, Italy, November 2006.

[6] S. Herman, "A particle filtering approach to joint passive radar tracking and target classification," Ph.D. dissertation, University of Illinois, 2002.

[7] B. H. Fleury, X. Yin, P. Jourdan, and A. Stucki, "High-resolution channel parameter estimation for communication systems equipped with antenna arrays," in *Proceedings of the 13th IFAC Symposium on System Identification (SYSID)*, no. ISC-379, Rotterdam, The Netherlands, 2003.

[8] X. Yin, T. Pedersen, N. Czink, and B. H. Fleury, "Parametric characterization and estimation of bi-azimuth and delay dispersion of path components," in *Proceedings of The First European Conference on Antennas and Propagation (EuCAP'06)*, Acropolis, Nice, France, November 2006.

[9] D. Fox, W. Burgard, F. Dellart, and S. Thrun, "Monte Carlo localization: Efficient position estimation for mobile robots," in *Proceedings of the 16th National Conference on Artificial Intelligence*, Orlando, FL, USA, 1999.

[10] M. Lenser, S.; Veloso, "Sensor resetting localization for poorly modelled mobile robots," *Robotics and Automation, 2000. Proceedings. ICRA '00. IEEE International Conference on*, vol. 2, pp. 1225–1232 vol.2, 2000.

[11] N. Czink, E. Bonek, X. Yin, and B. H. Fleury, "Cluster angular spreads in a MIMO indoor propagation environment," in *Proceedings of the 16th IEEE International Symposium on Personal, Indoor and Mobile Radio Communications (PIMRC'05)*, vol. 1, Berlin, Germany, September, 11-14 2005, pp. 664–668.

[12] E. Bonek, N. Czink, V. M. Holappa, M. Alatossava, L. Hentilä, J. Nuutinen, and A. Pal, "Indoor MIMO measurements at 2.55 and 5.25 GHz - a comparison of temporal and angular characteristics," in *Proceedings of the 15th IST Mobile Summit*, Myconos, Greece, June, 4-8 2006.

[13] X. Yin, B. H. Fleury, P. Jourdan, and A. Stucki, "Doppler frequency estimation for channel sounding using switched multiple transmit and receive antennae," in *Proceedings of the IEEE Global Communications Conference (Globecom'03)*, vol. 4, December 2003, pp. 2177–2181.